The DOI for this manuscript is doi: 10.1175/2010JCLI3738.1

Can the Increase in the Eddy Length Scale Under Global Warming Cause the Poleward Shift of the Jet Streams?

Joseph Kidston *

Princeton University, Princeton, USA

G. K. Vallis

Princeton University, Princeton, USA

S. M. Dean

National institute of Water and Atmospheric Research, Wellington, New Zealand

J. A. Renwick

National institute of Water and Atmospheric Research, Wellington, New Zealand

* *Corresponding author address:* Joseph Kidston, Geophysical Fluid Dynamics Laboratory, Forrestal Cam-

ABSTRACT

The question of whether an increase in the atmospheric eddy length scale may cause a poleward shift of the mid-latitude jet streams is addressed. An increase in the length scale of the eddy reduces its zonal phase-speed and so causes eddies to dissipate further from the jet core. If the eddy dissipation region on the poleward flank of the jet overlaps with the eddy source latitudes, shifting this dissipation to higher latitudes will alter which latitudes are a net source of baroclinic eddies, and hence the eddy-driven jet stream may shift polewards. This behavior does not affect the equatorward flank of the jet in the same way because the dissipation region on the equatorward flank is well separated from the source latitudes.

An experiment with a barotropic model is presented in which an increase in the length scale of a mid-latitude perturbation results in a poleward shift in the acceleration of the zonal flow. Initial investigations indicate that this behavior is also important in both observational data and the output of comprehensive general circulation models (GCMs). A simplified GCM is used to show that the latitude of the eddy-driven jet is well correlated with the eddy length scale. It is argued that the increase in the eddy length scale causes the poleward shift of the jet in these experiments, rather than vice-versa.

pus, Princeton University, NJ 08540

E-mail: jkidston@princeton.edu

1. Introduction

a. Jet stream movement

There is evidence of a poleward shift of the eddy-driven jet streams in recent decades, particularly in the southern hemisphere (Feldstein 2002; Marshall 2003; Ostermeier and Wallace 2003; Thompson et al. 2000; Trenberth et al. 2007). A large portion of the observed mid- to high-latitude temperature trends bear the signature of such a shift (Hurrell 1996; Thompson et al. 2000; Thompson and Solomon 2002; Trenberth et al. 2007). Events such as the European heatwave of 2003, the current drought in Southern Australia and the warming of the Antarctic peninsula have been at least partly attributed to these changes (Stott et al. 2004; Meehl and Tebaldi 2004; Murphy and Timbal 2008). Although it is not known with certainty whether the observed shift is a consequence of global warming, and so potentially a permanent feature, or whether it is a manifestation of natural variability, projections of the atmospheric response to increasing greenhouse gases (GHGs) indicate that the trend will continue throughout the 21st century (Fyfe et al. 1999; Meehl et al. 2007b; Yin 2005; Kushner et al. 2001; Bengtsson et al. 2006; Miller et al. 2006; Lorenz and DeWeaver 2007). The shift of the southern hemisphere eddy-driven jet stream is correlated with the projected expansion of the tropics (Lu et al. 2008). Given this, and that the mid-latitude jet streams are co-located with the storm tracks, the shift may be one of the most important circulation changes projected to occur under increasing GHGs. Even a small poleward shift in the surface westerlies could have large effects of the climate of many regions.

The poleward shift may be considered a robust response to increasing GHGs in that it occurs in almost all of the GCMs used in the IPCC AR4 report (Yin 2005). Furthermore, GCMs with highly simplified "physics" have been used to show that a poleward shift of the circulation is indeed a response to changes in the mean state expected under increasing GHGs, such as increasing tropopause height or tropospheric static stability (Lorenz and DeWeaver 2007; Frierson et al. 2006). However, there is also some debate over the likely magnitude of the shift. Son et al. (2008) have shown that if ozone recovery is properly taken into account, the poleward shift reverses sign during DJF. On the other hand, Johanson and Fu (2008) show that the AR4 models underestimate the observed poleward shift of the subtropical jet streams. Kidston and Gerber (2010) show that the inter-model variability in the magnitude of the shift is well correlated with biases in the control simulations. Understanding the underlying causes, and the inter-model variability, of such changes is paramount to having confidence in projections of such circulation changes under increasing GHGs. Other important and robust changes in the atmospheric circulation associated with a poleward shift of the jet include a decrease in the persistence of the jet (Kidston and Gerber 2010; Kidston et al. 2010b; Barnes et al. 2010), which may also be related to a broadening of the jet due to increased barotropic instability (Kidston and Vallis 2010)

b. Eddy driven jet dynamics

In the mid-latitudes the atmospheric circulation is dominated by large-scale ($\mathcal{O}$(5000 km)) eddies. The source of these eddies is baroclinic instability, which converts the available potential energy associated with a meridional temperature gradient into eddy kinetic energy. The time-mean location of these eddies defines the so-called storm tracks. In a hydrostatic and quasi-geostrophic atmosphere, a meridional eddy heat flux is synonymous with the vertical propagation of wave activity, and due to a westward phase tilt with height, this acts to transfer westerly momentum downwards. In the upper troposphere, the heat flux below can be thought of as acting to generate Rossby waves, which can radiate meridionally away from their source regions and break/dissipate. Because the zonal phase speed of a Rossby wave is westward (relative to the mean flow), the Rossby waves transport westerly momentum in the opposite direction to their meridional group velocity, and so converge westerly momentum into their source latitudes. Thus the meridional radiation of wave activity aloft converges westerly momentum into the source latitudes, and the heat flux barotropizes that westerly momentum; a barotropic, eddy-driven jet stream is generated at latitudes that are a *net source of baroclinic eddies*. An alternative way of thinking of this picture is that waves irreversibly mix potential vorticity (PV) in the regions where they break and dissipate. This increases the meridional gradient of PV in the latitudes with no wave breaking (i.e. the wave source latitudes), thereby making a PV "staircase". A PV gradient acts as a restoring force, encouraging Rossby wave motion, thereby discouraging wave breaking and mixing. Thus once the PV gradient increases in the source region, it will tend to encourage any further mixing to occur elsewhere, thereby encouraging a PV staircase. A maximum in the PV gradient corresponds to a maximum in the zonal wind-speed, and so a PV staircase forms zonal jets (Dritschel and McIntyre 2008). Thereby waves radiating away from their source region form a PV staircase, which from the momentum point of view creates an up-gradient flux of zonal momentum and forms zonal jets.

There is no universally accepted mechanism for the cause of the poleward shift of the jet streams under global warming. Hartmann et al. (2000) suggested that it may be caused by a decrease in the index of refraction at high latitudes. This would encourage equatorward propagation of wave activity, which is associated with anticyclonic wavebreaking, and the jet being displaced towards the pole (Thorncroft et al. 1993).

Chen et al. (2007, 2008); Chen and Held (2007) have argued that the increase in the eddy zonal phase-speed (c) caused by an increase in the mid-latitude zonal-mean zonal wind-speed ($\bar{u}$) is important. Linear theory predicts that eddies dissipate where $\bar{u} = c$, and observations show this to roughly hold true (Randel and Held 1991). If $\bar{u}$ changes relatively little in low-latitudes, then equatorward propagating eddies must dissipate at higher latitudes as c increases. On the poleward flank of this eddy dissipation region, there is sinking (and adiabatic warming) driven by the mean meridional overturning. If the dissipation (and so the sinking and warming) moves polewards, it might be expected that the region where the meridional temperature gradient is highest also moves poleward. The region of baroclinic instability, and the eddy-driven jet stream may shift accordingly.

Frierson et al. (2006) and Lu et al. (2008) have suggested that the increase in water vapour content of the atmosphere, expected in warmer climates, increases the dry static stability at low-latitudes relative to high-latitudes. Because a statically stable atmosphere resists the vertical motions associated with baroclinic instability, this may shift the eddy source region polewards.

In this paper we argue that the increase in the eddy length scale associated with increasing GHGs (Kidston et al. 2010a) may be important for shifting the jet polewards. There has been previous work that is broadly consistent with this idea; for example, Govindasamy and Garner (1997) found that in a baroclinic eddy lifecycle experiment waves of larger spatial extent break preferentially anticyclonically, which is known to encourage a poleward displaced jet. This is because of an asymmetry in the normal mode structure between zonal wavenumber six (k-6) and k-8. The k-6 normal mode was tilted so as to increase the anticyclonic shear on the equatorward side. This induced preferential anticyclonic wavebreaking when compared with k-8. Orlanski (2003) also found that anticyclonic wavebreaking is preferred for longer waves, but focused on a different mechanism. A shallow water model was used to show that as the eddy amplitude increased and the evolution became non-linear, cyclonic wave breaking started to dominate over anticyclonic wavebreaking. This was due to the cyclonic perturbations achieving higher magnitude relative vorticity than the anticyclonic perturbations (which are limited by inertial instability). This effect becomes important for short waves before long waves because the magnitude of the relative vorticity increases with the wavenumber.

Here we propose a different and arguably simpler mechanism whereby an increase in the eddy length scale can effect a poleward shift of the eddy-driven jet. An increase in the eddy length scale decreases the intrinsic eddy phase-speed, as planetary vorticity advection increases compared to relative vorticity advection. If $\bar{u}$ is approximately unchanged, a reduction in c means that eddies dissipate further from the jet core. If the dissipation region is well separated from the source region, this would not affect which latitudes are a net source of eddies. However, suppose that the breaking region on the *poleward* flank of eddy driven jet overlaps with the generation region where baroclinic instability occurs. As the dissipation region on the poleward flank moves to higher latitudes, regions will effectively transition from being a net sink to a net source of eddies, and the eddy-driven jet will move polewards. This behavior may be less important on the equatorward flank because here the dissipation region is already well separated from the source region. This mechanism is illustrated in Figure 1. The blue line shows the probability of exciting an eddy. It corresponds to the likelihood of baroclinic instability providing a stirring. The waves that this stirring excites are able to propagate meridionally, so that the regions where the waves are likely to dissipate are latitudinally separate, shown by the red lines for the control (solid), and future (dashed). Because the waves propagate meridionally, they converge westerly momentum into the source latitudes, and diverge westerly momentum out of the decay regions. The sum of the red and blue lines gives the *net source of eddy activity*, and therefore the net convergence of zonal momentum. This determines the time-mean zonal wind-speed (black lines), which is simply the arithmetic sum of the blue and red lines. In the future, the dissipation moves further from the source region. Moving both source regions further from the jet results in a broader, and poleward shifted jet. This is a result of the source and sink regions overlapped being overlapped on the poleward flank. (We do not consider *why* the source region may be overlapped with the sink region on the poleward flank more than on the equatorward flank. It is possible that the existence of a sub-tropical jet means that waves propagate further meridionally before reaching their critical latitude on the equatorward side.) The relationship between this theory and those outlined above is discussed.

[Figure 1 about here.]

2. Data and methods

a. Data sources

In order to determine the generality of the results, this study aims to show similarity between observational data, output from a state-of-the-art GCM, and output from a simplified GCM. The observational data are the NCEP/NCAR reanalyses (Kalnay et al. 1996) for 1979-2007. As state-of-the-art model output, the GCMs used in the World Climate Research Programme's (WCRP's) Coupled Model Intercomparison Project phase 3 (CMIP3) multi-model dataset (Meehl et al. 2007a) are used. The caption for Figure 2 gives a list of the models used for calculating the ensemble-mean diagnostics. The full GCM diagnostics that are not an ensemble-mean are from the Geophysical Fluid Dynamics Laboratory (GFDL) gfdl_cm2_1 model (Anderson et al. 2004). For the simplified GCM, the GFDL spectral dynamical core developed for the intercomparison in Held and Suarez (1994) is used. The model is set up with triangular truncation at T42, and 20 levels evenly spaced in fraction of surface pressure (σ). The forcings are simplified in that they consist only of a Newtonian relaxation to an equilibrium temperature (T_{eq}) field; Rayleigh friction (below $\sigma = 0.7$); and hyperdiffusivity to remove energy at small scales. The model control run was set up as in Held and Suarez (1994); control values of key variables (that were used to manipulate the eddy length scale) were: the equator-pole T_{eq} difference was 60 K at the surface; the isothermal stratospheric T_{eq} was 200 K; and the hyperdiffusivity operator was ∇^8 with a coefficient so that the smallest scales were damped with an e-folding time of 1/10 days.

We also present output from an experiment using a barotropic model. The model solves the non-divergent vorticity equation on the sphere and is the same as used in Held and Phillips (1987). The experiment is an initial value perturbation, which is allowed to evolve for 20 days, the only dissipation being hyperdiffusivity, the coefficients the same as in the idealized baroclinic GCM. The flow on which the perturbation evolves is taken from Held and Phillips (1987) and is supposed to be a realistic representation of the upper-tropospheric wintertime flow. The initial perturbation is a wave in the mid-latitudes, which then propagates meridionally with time. The initial perturbation has zonal wavenumber k_o, is centered at 45 degrees latitude, and has a meridional structure that decays exponentially in latitude, with a half width of 15 degrees;

$$\zeta' = A_o e^{-[(\phi-45)/15]^2} \cos k_o \theta \tag{1}$$

where ϕ is latitude and θ is longitude in radians. The zonal wavenumber was set to either 5 or 7 to change the spatial scale. The magnitude of the perturbation, A_o was set to 8×10^{-8} s^{-1} to keep the perturbation very small and therefore linear, although the results were qualitatively unchanged when the amplitude of the perturbation was increased.

b. Spectral decomposition

We decompose both the meridional component of the eddy kinetic energy (EKE) and the momentum flux, ($\overline{u'v'}$, where the overline represents zonal averaging the primes departures therefrom) into wavenumber contributions in the standard way; at constant latitude, the meridional velocity $v(\lambda, t)$ is decomposed into Fourier components around latitude circles so that

$$v(\lambda, t) = \sum_k \mathrm{Re}\left[\tilde{V}_k(t) e^{ik\lambda}\right] \tag{2}$$

where the real and imaginary parts of $\tilde{V}_k(t)$ are the cosine and sine coefficients respectively. The EKE at any given k is then $0.5\times|\tilde{V}_k(t)|^2$ and the momentum flux of any k is $0.5\times\mathrm{Re}\left[\tilde{V}_k(t)\tilde{U}_k^*(t)\right]$ where the * denotes the complex conjugate. The EKE has been calculated for the meridional component, although the results are unchanged when the zonal component is included. The energy containing k at each ϕ was calculated as

$$\bar{k}(\phi, t) = \frac{\sum_k k \times |\tilde{V}_k(t)|^2}{\sum_k |\tilde{V}_k(t)|^2} \tag{3}$$

and the wavelength, or eddy length scale, is then $\bar{\lambda}(\phi, t) = 2\pi a \cos(\phi)/\bar{k}(\phi, t)$, where a is the Earth's radius. The time-mean eddy length scale is denoted $\bar{L}(\phi)$.

The momentum flux was also decomposed into contributions from different phase-speeds. This was accomplished as in Hayashi (1979), Randel and Held (1991) and Chen et al. (2007). The real and imaginary components of $\tilde{V}_k(t)$ can each be Fourier decomposed in time such that

$$\mathrm{Re}\left[\tilde{V}_k(t)\right] = \sum_\omega \mathrm{Re}\left[\tilde{A}_{k,\omega} \mathrm{e}^{i\omega t}\right] \tag{4}$$

$$\mathrm{Im}\left[\tilde{V}_k(t)\right] = \sum_\omega \mathrm{Re}\left[\tilde{B}_{k,\omega} \mathrm{e}^{i\omega t}\right] \tag{5}$$

After the same decomposition for the real and imaginary part of $\tilde{U}_k(t)$, we obtain an expression for the cospectral power density as a function of frequency and wavenumber at each latitude: If

$$A = \mathrm{Re}\tilde{A}_{k,\omega}; \quad a = \mathrm{Im}\tilde{A}_{k,\omega}; \quad B = \mathrm{Re}\tilde{B}_{k,\omega}; \quad b = \mathrm{Im}\tilde{B}_{k,\omega} \tag{6}$$

then the cospectral density as a function of wavenumber and frequency is

$$K_{k,\pm\omega} = 2\left[(A^v \mp b^v)(A^u \mp b^u) + (\mp a^v - B^v)(\mp a^u - B^u)\right] \tag{7}$$

where the superscripts refer to the original field.

The interpolation into phase-speed space is defined so that total power is conserved:

$$K_{k,\pm\omega}\Delta\omega = K_{k,\pm c}\Delta c \tag{8}$$

c. *Other diagnostics*

The momentum flux convergence was calculated as

$$\frac{1}{a\cos^2\phi}\frac{\partial}{\partial\phi}\overline{u'v'}\cos^2\phi \tag{9}$$

The buoyancy frequency between 850 and 600 hPa is used to quantify the dry static stability, and is calculated as $N = \sqrt{g\partial\ln(\theta)/\partial z}$ where g is gravity, θ is the potential temperature, and z is height. The hydrostatic approximation was used to calculate N for model output on constant pressure levels.

The internal variability in the latitude of the eddy-driven jet was indexed as the principle component (PC) of the first empirical orthoganol function (EOF) of the zonal-mean zonal wind-speed anomaly ($\bar{u}'$), latitude weighted to account for converging meridians towards the poles. We calculate the EOF at 300 hPa. However, given that the annular modes are equivalent barotropic, PC1 from different heights is well correlated, and so the choice of level is unimportant. For the NCEP/NCAR data and the GCM output, the anomalies were defined as departures from the calendar month mean, smoothed to remove discrete jumps between months. For the simplified GCM the anomalies were defined as departure from the time-mean.

3. Results

a. *An increase in the eddy length scale under global warming*

The increase in the eddy length scale in simulations of future climate that has been documented in Kidston et al. (2010a) is summarized in Figure 2. The shading shows that in the ensemble-mean, the change in the EKE in the future simulations shows both a poleward shift in the eddy activity, and an increase in the wavelength of the energy containing eddies. The ensemble-mean $\bar{L}(\phi)$ shows a clear increase (white lines). This increase is robust in that it occurs in both hemispheres and in every model (Kidston et al. 2010a).

[Figure 2 about here.]

b. *The cause of the increase in the eddy length scale*

The cause of the increase in $L(\phi)$ is unclear. In this section it will be argued that the poleward shift of the jet does not cause the increase in $L(\phi)$. Kidston et al. (2010a) showed that the inter-model variability of the increase in L is well correlated with the increase in N. This is what would be expected if the Rossby radius ($L_R = NH/f$ where f is the Corriolis parameter and H a scale height) were the controlling influence on the eddy length scale. On the other hand, if the Rhines scale ($L_\beta = \sqrt{U'/\beta}$ where U' is the eddy velocity and β the environmental vorticity gradient) is dominant, one might expect a poleward shift of the eddy source region to cause the increase in the eddy length scale, as β decreases towards the pole.

To investigate whether the latitude of the jet determines the eddy length scale, we consider the co-variability of the length scale with the internal variability of the zonal-mean zonal wind, or annular mode. The poleward shift of the zonal winds under increasing GHGs projects onto the annular modes (Yin 2005). Therefore an investigation of the impact of variations in the annular mode on the eddy length scale is the first step in answering the question of whether the poleward shift of the jet causes the increase in L. The regression coefficient for Ł(ϕ) and PC1 is shown in Figure 3 for the various data sources. Also shown is the regression coefficient for $\bar{u}'$ at 300 hPa (solid line). In all cases the first EOF represents a meridional vacillation of the eddy driven jet; the mid-latitude node of the regression coefficients for $\bar{u}'$ coincides with the time-mean jet position (not shown). The regression coefficients for $\bar{u}'$ for the NCEP/NCAR reanalysis and gfdl_cm2_1 are very similar; the main feature is an increase in $\bar{u}'$ at 55°S and a decrease in $\bar{u}'$ at 35°S. The simplified GCM has an additional feature, the dipolar vacillation of $\bar{u}$ in the tropics, which approximately corresponds to a shift of the subtropical jet stream (not shown). In all cases the changes in eddy length scale mirror those in the zonal-mean zonal wind, but they are latitude shifted so that the extrema are a few degrees towards the equator. There is no hemisphere-wide increase in the eddy length-scale (as is seen in Figure 2). It may be argued that the time scale of the variability in the real atmosphere is too fast to allow the eddy length scale to respond to the change in jet position. However, in the models the time-scale of variability is much longer (Gerber and Vallis 2007; Gerber et al. 2008); the e-folding period of PC1 for the observations is 11.1 day, the GFDL CM2.1 is 12 days, and the simplified GCM output is 35.2 days. Kidston et al. (2010b) has shown that there is a clear poleward shift in the latitude of eddy-generation associated with the positive phase of the annular mode of the simplified GCM with the configuration shown here. Thus the time-scale of the annular mode in the simplified GCM is likely long enough for any hypothesized hemisphere-wide increase in the eddy length-scale associated with a poleward shift of the jet to manifest. That this is not observed suggests that the latitude of the baroclinic source region is not a strong control on the global mean eddy length scale.

[Figure 3 about here.]

Kidston et al. (2010a) found that the inter-model variability in the increase of the eddy length scale in the AR4 models was correlated with the increase in the dry static stability. Frierson (2006) has shown that under increasing GHGs there is a hemisphere-wide increase in N throughout the troposphere, apart from close to the surface at high northern latitudes during boreal summer. This would be consistent with the hemisphere-wide increase in L shown in Figure 2. Figure 4 shows the changes in N associated with the annular mode. Near the top of the troposphere there is an increase in N at high latitudes associated with a poleward shifted storm track. This positive anomaly tilts equatorwards as it extends towards the surface. Equatorward of this there is a negative and a positive anomaly, so that in the mid-troposphere there is an approximately tri-polar pattern. To emphasize that the mid-latitude feature represents a poleward shift of the climatology, the difference between N and the mean N at a particular pressure level (N - $\bar{N}_p$) is also contoured in Figure 4 (b). The contours show a lobe of high static stability starting near 30S at the surface and tilting poleward with height. (This feature coincides well with the poleward tilt with height of the time-mean storm track, or eddy heat flux (not shown)). Thus the mid-latitude changes in N are seen to represent a poleward shift of the climatology in the dry limit. Attribution of the changes in the eddy length scale (seen in Figure 3) to changes in N is complicated by the poleward phase tilt with height of the N anomalies. Nonetheless, the changes in static stability from roughly 800-500 hPa are consistent with the change in length scale seen at 300 hPa. It is reasonable to suppose that a growing baroclinic eddy would be most strongly affected by N at these levels.

[Figure 4 about here.]

It could be argued that the changes in $L(\phi)$ associated with a positive PC1 are consistent with an L_β scaling; there is a poleward shift in the EKE when the eddy-driven jet is displaced towards the pole. However, this argument is flawed because the changes in the EKE more closely track those of $\bar{u}$, and are not phase shifted in the same manner as the changes in $L(\phi)$. Furthermore, in the CMIP3 future simulations, there is no consistency in the sign of the change in EKE. The conclusion then is that both the variability in $L(\phi)$, and the changes in $L(\phi)$ with increasing GHGs, are well captured by changes in the dry static stability. This implies that L_R is a more appropriate scaling for the variations in the eddy length scale than L_β, and so a poleward shift of the jet would not intrinsically cause the eddy length scale to increase.

c. The consequences of the increase in the eddy length scale

In so far as linear theory is valid, the eddy length scale is of first order importance for determining wave-mean flow interaction; both the height and latitude at which waves break are influenced by the spatial scale of the wave. For a given amplitude wave, an increase in the length scale decreases the relative vorticity advection, which would cause c to decrease. To investigate whether the linear dispersion relation is at least qualitatively relevant for realistic baroclinic eddies, a decomposition of the meridional component of the EKE is shown in Figure 5 as a funciton of k and c. The data are from the gfdl_cm2_1 model, and are on the 300 hPa surface, at the approximate latitude of the eddy-driven jet of 51°S. As the length scale decreases (k increases) the phase-speed of the energy-containing eddies rapidly increases, consistent with the linear theory. Therefore one impact of an increase in L would be a decrease in c, at least relative to the mean flow.

[Figure 5 about here.]

It is known that under increasing GHGs the absolute eddy phase-speed (relative to the ground) increases (Chen and Held 2007). However, an increase in the eddy length scale would suggest a decrease in the phase-speed relative to the mean flow. To investigate this, Figure 6 shows the momentum flux convergence, as a function phase-speed relative to the zonal flow, and latitude. The phase-speed decomposition was done in the standard way (described in the Data and Methods section), and the zonal-mean zonal wind was then subtracted from the absolute phase-speed to give the phase-speed relative to the mean flow.

Figure 6 (a) shows data for the 20$^{\text{th}}$ century control run of the gfdl_cm2_1 model. The momentum flux convergence at negative phase-speeds in the mid-latitudes indicates that at latitudes that are a source of eddy activity, the eddies propagate westward relative to the mean flow. The momentum flux convergence peaks at speeds of -30 to -35 ms^{-2} and at latitudes just poleward of 50°S.

The momentum flux divergence at high- and low-latitudes indicates a net sink of eddies. At high-latitudes the eddies dissipate at roughly -15 ms^{-1} relative to the mean flow, which seems rather fast considering that the linear critical latitude is located where the eddy zonal phase-speed matches the wind-speed. However, this may be a complication of the 3-D nature of eddies: The maximum eddy driving of the mean flow at high-latitude occurs at 500-400 hPa (not shown), which is roughly the tropopause level at high-latitude. At these levels, the wind-speed is lower than at 300 hPa due to the meridional temperature gradient. Hence the eddies may be dissipating at roughly their critical latitude lower down in the atmosphere. The barotropic nature of the eddies toward the end of the lifecycle means that above the dynamically dominant level, the momentum fluxes occur while the eddy is still moving westward relative to the mean flow.

On the equatorward side eddies dissipate at roughly -10 ms^{-1} relative to the mean flow. This is close to the critical latitude. There is a tilt to this dissipation region, so that the dissipation tends to occur at zero (relative) phase-speed at lower latitudes. It is possible that this tilt is also explained by the same 3D dynamics just postulated for the poleward flank: The tropopause is above 300 hPa at very low-latitudes, and so eddies that break on the tropopause in that region, just *before* their critical latitude, will appear to actually reach their critical latitude lower down, where the wind-speed is reduced.

Generally speaking the picture is consistent with the view that the eddy life-cycle consists of eddies propagating upward to the tropopause, and then propagating meridionally and dissipating slightly before reaching their critical latitude.

Figure 6 (b) is the same as panel (a) but for data at the end of the simulated 21$^{\text{st}}$ century in the A2 scenario. The picture is approximately the same, but the maximum acceleration in mid-latitudes occurs at speeds of -35 to -40 ms^{-1}, and at latitudes around 55°S: I.e. the westward phase-speed relative to the mean flow has increased and the source region has moved slightly poleward. This is confirmed in Figure 6 (c), which shows the difference between the future and the control. At the source region, eddies are moving westward faster relative to the mean flow. The dissipation region at low-latitude shows very little change, indicating that eddies still dissipate at roughly their critical latitude. On the poleward flank, the dissipation occurs at relative-speeds that are closer to zero, i.e. the eddies get closer to their critical latitude (at 300 hPa). This could be because the tropoause rises in these simulations, and so the dynamically important level for wave breaking rises closer to the 300 hPa level on the poleward side.

[Figure 6 about here.]

So associated with the poleward shift in the eddy source region is an increase in the westward phase-speed of the eddies relative to the mean flow. The increase in the speed of the mean flow is greater than the change in the relative phase-speed, and so the absolute phase-speed increases (Chen and Held 2007). However, given that waves dissipate roughly where $\bar{u} = c$, if eddies have a slower phase-speed relative to the mean flow then eddies may propagate further meridionally away from a jet before dissipating (if to first order the mean flow changes are the same everywhere). Figure 6 is consistent with this; there is no obvious change in the dissipation latitudes on the equatorward side, whereas the source region moves poleward, so that the meridional distance traveled by an eddy increases.

To illustrate the importance of eddies propagating further from a jet, results from experiment with the barotropic vorticity equation on the sphere are shown in Figure 7. The experiment was an initial value perturbation in the mid-latitudes which was allowed to evolve freely. The zonal-mean zonal wind for day 1 of the experiment is shown in Figure 7 (a). Because the initial perturbation was of small amplitude, $\bar{u}$ did not change significantly over the course of the experiment. The total eddy vorticity flux ($\overline{v'\zeta'}$; equivalently the divergence of the meridional flux of westerly momentum) is shown in the lower panel. The positive values in the mid-latitudes are expected if the initial distribution of pseudomomentum, or wave activity, propagates away to other latitudes. This imparts a net acceleration on the mean flow in the source region. The regions where $\overline{v'\zeta'}$ is negative indicate net deposition of wave activity, which acts to decelerate the mean flow. For both experiments there is deposition of pseudomomentum at both high- and low-latitudes. Both of the dissipation regions for the k-5 wave are further from the source region than those of the k-7 wave. This is expected from linear theory, given that the k-5 has a reduced eastward phase-speed, and the waves dissipate where $u = c$. On the equatorward side the acceleration of the zonal flow (in the source region) is mostly unaffected by this difference as the dissipation region is well separated from the source region. Conversely, on the poleward side, the dissipation of the k-7 wave clearly overlaps the region where wave activity was initiated, and acceleration of the zonal flow is diminished relative to the k-5 case. Latitudes that would be net sources of wave activity in the k-5 case are a net sink in the k-7 case, and the latitude of maximum acceleration of the zonal flow is shifted equatorward. The picture is very similar to that suggested in Figure 1. It is clear that if a forced-dissipative experiment were set up with a time-mean jet similar to that shown in Figure 7 (a), an increase in the eddy length scale would act to induce a poleward shift of the jet. This is the mechanism that may induce a poleward shift of the jet following an increase in the eddy length scale.

[Figure 7 about here.]

It is trivial to set up a jet in this model where this behavior is not seen; if there were only a turning latitude on the poleward side, rather than a critical latitude, there would be no dissipation on the poleward side, and no possibility of this behavior arising. For this mechanism to be relevant to the real world a number of conditions need to be satisfied; there must be dissipation on the poleward side; this must be overlapped with the stirring region more than on the equatorward side; and the linear theory should be valid to the point that an increase in the length scale is associated with dissipation further from the source region.

To examine whether similar behavior is seen in more realistic jets, the time-mean upper tropospheric $\overline{v'\zeta'}$ for the various data sources is shown as a function of latitude and wavelength in Figure 8. In all three data sets there is momentum flux convergence in mid-latitudes and divergence on the flanks of the mid-latitudes. If the values were summed over $\lambda(\phi)$ there would be more dissipation on the equatorward side than the poleward side, consistent with the picture that most wave activity propagates equatorward (Edmon et al. 1980). The dissipation region on the poleward flank has a poleward tilt with increasing length scale, and the dissipation region on the equatorward flank has an equatorward tilt with increasing length scale. Both of these features are consistent with the notion that longer waves dissipate further from the jet, as expected because they have lower phase-speed. The eddy source region shows a more complicated dependence on length scale, but as the length scale increases from 5000 km to 10000 km, there is a subtle poleward tilt with increasing length scale. This implies that in the climatology, longer waves accelerate the flow further poleward. If one traces the dashed line at 65S in Figure 8 from low to high $\lambda(\phi)$, the region transitions from being a net sink region to a net source region. Thus, all else being equal, an increase in the eddy length scale may change this region from a net sink to a net source of wave activity, and act to shift the jet polewards.

[Figure 8 about here.]

To emphasize the conclusion that longer waves accelerate the flow further poleward, Figure 9 shows a slice of the data shown in Figure 8. The wavelength at which the slice is taken is detailed in the Figure legend. The wavelengths were chosen such that the lower value corresponds to wavelengths that are projected to account for less (hemispherically integrated) kinetic energy in the future, and the higher value corresponds to wavelengths that are projected to account for more kinetic energy in the future (Figure 2). In all of the datasets, the peak in the acceleration is further poleward for longer waves, thereby confirming the conclusion drawn from Figure 8 that longer waves accelerate the flow further poleward. Thus it appears that the eddy dissipation characteristics in the observations and the GCMs are similar to the barotropic model; long waves accelerate the zonal flow further poleward than short waves.

[Figure 9 about here.]

To confirm that the dependence of the latitude of dissipation on length scale is in fact a phase speed effect, the momentum flux convergence at approximately 300 hPa is given as a function of phase-speed in Figure 10. Only positive phase-speeds are shown because all of the dissipation on the poleward flank occurs at $c > 0$. Randel and Held (1991) showed that the vast majority of the cospectral power is in waves with $c > 0$. It is clear that for all of the data sets, the dissipation regions on both sides of the jet tilt towards the mid-latitude source region for increasing c. Thus faster waves dissipate closer to the jet core, which as theory suggests, and Figures 5 and 8 confirm, corresponds to shorter waves. This behavior has been noted for the equatorward dissipation region by Randel and Held (1991), and Chen et al. (2007), Chen and Held (2007) and Chen et al. (2008) have suggested that this may imply that an increase in phase-speed could cause a poleward shift of the jet. Here it has been suggested that a *decrease* in the (intrinsic) phase-speed, caused by an increase in the length scale, may cause a poleward shift of the jet. The apparent conflict with the works cited is discussed below.

[Figure 10 about here.]

As previously discussed, for a decrease in the intrinsic phase-speed to cause a poleward shift of the jet, it is necessary that the eddy dissipation region on the poleward flank of the jet is overlapped with the source region to a greater extent than that on the equatorward flank. To investigate this the time-mean near-surface $\bar{u}$, and the vertically averaged eddy heat flux is shown in Figure 11. As previously discussed, the latitudes where $\bar{u}$ is positive indicate regions that are net baroclinic eddy source regions, and the latitudes there $\bar{u}$ is negative indicate net dissipation regions. The vertically averaged eddy heat flux can be taken as an indicator of where baroclinic instability stirs the flow, and eddy generation occurs. At the latitudes on the equatorward flank of the jet where there are the strongest surface easterlies (approximately 15°S), the vertically integrated eddy heat flux is very nearly zero, indicating that the eddy dissipation region on the equatorward flank is not overlapped with the source region. Conversely, at the latitudes on the poleward flank where there are the strongest surface easterlies (approximately 70°S), there is still substantial vertically integrated eddy heat flux. This suggests that the dissipation on the poleward flank is more overlapped with the eddy source region than that on the equatorward flank. It may make sense that the high-latitude easterlies are less strong than those at low-latitudes, as the stirring by baroclinic instability on the poleward flank of the jet is in competition with the dissipation. The fact that the dissipation region on the poleward flank is overlapped with the source region to a greater extent than that on the equatorward side is further empirical evidence that decreasing the intrinsic eddy phase-speed may cause the surface westerlies to shift polewards.

[Figure 11 about here.]

d. Simplified GCM experiments

The simplified GCM has been used to investigate whether a change in the eddy length scale impacts the latitude of the jet stream. The aim was to manipulate the basic state so that the eddy length scale was impacted, and investigate whether the latitude of the jet stream responded as expected. The basic state was manipulated in various ways. The first was to increase the tropopause height. This is expected to increase the eddy length scale if the H contained in L_R corresponds to the tropopause height. Increasing the tropopause height may also be expected to increase the eddy length scale if it causes the eddies to penetrate deeper vertically, and the aspect ratio of the eddies is fixed (Held 1982). As in other studies (Lorenz and DeWeaver 2007), the tropopause height was increased in the model by decreasing the stratospheric T_{eq}. In the increased tropopause height experiment (named $H_{increased}$) the stratospheric T_{eq} was set to 197 K, 3 K colder than in the control run experiment ($Control$). As expected, the actual model air temperature (T) in the stratosphere was decreased in $H_{increased}$ relative to $Control$ (Figure 12 (a)). Relative to $Control$, $H_{increased}$ shows a shift to longer λ (Figure 12 (d)). An accompanying poleward shift of the eddy-driven jet is seen in Figure 12 (g). Previous studies have pointed out that increasing H causes a poleward shift of the jet (Haigh et al. 2005; Lorenz and DeWeaver 2007), and Williams (2006) also noted the accompanying increase in the eddy length scale, but the dynamical mechanism hypothesized here was not suggested.

[Figure 12 about here.]

A second manipulation that was imposed in order to increase the eddy length scale was an increase in the equilibrium static stability. In order to increase N in the model, T_{eq} was decreased near the surface rather than increased higher up (as happens under global warming), in order to keep H approximately constant. This run is named $N_{increased}$. The temperature anomaly in $N_{increased}$ is dispersed (Figure 12 (b)), a result of dynamics, making the troposphere generally more statically stable. There is also an increase in the meridional temperature gradient ($|\partial T/\partial y|$), possibly due to baroclinic adjustment. This is unfortunate as separating the influence of N and $|\partial T/\partial y|$ becomes somewhat intractable in this model. Figure 12 (e) shows that relative to $Control$, $N_{increased}$ exhibits an increase in eddy length scale. Given that lines of constant temperature difference between $N_{increased}$ and $Control$ are *primarily* horizontal (Figure 12 (b)), we attribute the difference between the runs at least partly to increased N.

A third change of state that would be expected to induce larger eddies is an increase in $|\partial T/\partial y|$ so there is more available potential energy, and eddies are better able to overcome the Earth's vorticity gradient (β). This may be due to changes in the fastest growing normal mode, as in the two-layer or Charney model (Vallis 2006), or due to a nonlinear turbulent cascade of energy to larger spatial scales (Rhines 1975; Vallis and Maltrud 1993; Welch and Tung 1998; Frierson et al. 2006). In order to increase $|\partial T/\partial y|$ in the model, the e-folding period of the Newtonian cooling constant was decreased. This run is named $|\partial T/\partial y|_{increased}$. Figure 12 (c) shows that $|\partial T/\partial y|$ was indeed increased in this run (because T was closer to T_{eq} than in *Control*). This method was chosen over increasing $|\partial T_{eq}/\partial y|$ because, as can be seen from Figure 12 (c), it gave minimal change in N. As is seen in Figure 12 (f) and (i), the eddy length scale increased in $|\partial T/\partial y|_{increased}$, and there was a poleward shift of the eddy-driven jet.

The climatological variation of the eddy length scale with latitude in *Control* shown in Figure 12 (d) provides further insight as to whether an increase in the eddy length scale is the cause of the poleward shifts shown in Figure 12 (g)-(i). As in the CMIP3 models (Figure 2 (a)) the mean wavelength decreases towards the pole. An increase in eddy length scale that is accompanied by a poleward shift of the jet varies in the opposite sense to this climatology, and may therefore be suggestive of non-trivial underlying dynamics.

In order to more rigorously asses whether the eddy length scale influences the latitude of the jet in this model, experiments were conducted where the rate at which energy is removed at small scales, via the hyperdiffusivity operator, was varied. Table 1 shows that when the damping is relatively weak (the denominator in the damping value is large), the length scale is reduced. (The length scale was calculated by simply averaging $L(\phi)$ between 70° and 25°S. The values were not variance weighted because of the climatological decrease in $L(\phi)$ toward the pole (Figure 12 (d)), so variance weighting in the presence of a poleward shift of EKE could result in a decrease in the average value in the presence of an increase at every latitude). The relationship between the damping and the eddy length scale is expected as when the damping is weak there is more EKE at the small scales affected by the hyperdiffusivity operator. The eddy length scale increases monotonically as the damping increases.

It appears that there is some noise in the values of the jet latitude shown in Table 1. It is possible that if the integration time was increased the noise would reduce and the variation of jet latitude with damping time would be monotonic. Nonetheless, Figure 13 shows that the eddy-driven jet tends to be located towards the pole when the eddy length scale is large (the damping is strong). The correlation between the jet latitude and the eddy length scale is -0.78. Given that this relationship is not simply consistent with the climatological variation of wavelength with latitude, and as we have argued, there exists a physical mechanism for such a relationship, Figure 13 is consistent with the hypothesis that the increased eddy length scale may cause a poleward shift of the eddy-driven jet stream in this model.

[Table 1 about here.]

[Figure 13 about here.]

4. Discussion and conclusions

In this paper we have proposed a mechanism whereby an increase in the eddy length sale — such as that projected to occur under increasing GHGs — can lead to a poleward shift of the eddy-driven jet. Such a shift is also projected to occur in a large number of simulations of a warming climate. In brief, the mechanism is as follows. An increase in the eddy length scale causes a decrease in the intrinsic eddy zonal phase-speed. This will cause eddies to dissipate further from the jet core. If the dissipation region initially overlaps with the source region, (as it does on the poleward side of the baroclinically active region in midlatitudes), then changing the latitude of eddy dissipation will alter which latitudes are a net source of eddies. In contrast, the dissipation region on the equatorward flank of the jet is well separated from the source region so the mechanism has little effect there. The result is that an increase in the eddy length scale, or decrease in the intrinsic phase-speed, may cause a poleward shift of the mid-latitude eddy-driven jet and a poleward shift of the surface westerlies.

The dynamics we have proposed were found to be relevant in an initial value perturbation experiment with the barotropic momentum equation on the sphere. Furthermore it appeared that in the climatologies of both the observations, and the complex and simplified GCMs, longer waves accelerated the flow further poleward than short waves, which is consistent with this mechanism being relevant to those data. The simplified GCM was used to show that when the basic state was manipulated in such a way as to impact the eddy length scale, the latitude of the eddy-driven jet responded in a way consistent with these dynamics; when the length scale was increased, the jet moved polewards. The internal variability of the model was used to argue that the latitude of the jet is not a strong control on the eddy length scale, and so the increase in the eddy length scale is not caused by the shift of the jet. The mechanism proposed here predicts that the latitude of the jet will shift in association with a change in latitude of the westerlies on the poleward (rather than equatorward) flank. The authors have a paper in preparation that shows that this does indeed seem to be the case.

In addressing the relationship with this work and that of Chen et al., we note that the two mechanisms need not be mutually exclusive. The mechanism proposed by Chen et al. is based on a relative increase in the angular wind-speed in the mid-latitudes relative to low-latitudes. Consider the situation where the angular wind-speed increases at both mid- *and* high-latitudes relative to the low-latitudes. If the intrinsic phase-speed remained constant, the critical latitude on the poleward flank would not change location, but the critical latitude on the equatorward side would move poleward. Then consider the case where the zonal wind-speed changes described above are accompanied by a decrease in the *intrinsic* phase-speed (or an increase in the eddy length scale). Now the critical latitude on *both* sides of the jet may move poleward. In this case the increase in c relative to the sub-tropical $\bar{u}$ causes a poleward shift of the eddy dissipation on the equatorward flank, and the decrease in c relative to the high-latitude $\bar{u}$ causes a poleward shift of the eddy dissipation on the poleward flank. The Chen et al work was partially supported by the shallow water model in Chen (2007), where results showed than an increase in the eddy zonal phase-speed caused a poleward shift of the jet. It is worth pointing out that the shallow water model used therein did not have significant breaking on the poleward flank (not shown), which is crucial to the mechanism proposed here. Furthermore, experiments with the dynamical core in which the timescale of surface friction is increased, which have been used to argue that an increase in phase-speed causes a poleward shift of the jet (Chen et al. 2007), in fact also exhibit an increase in the eddy length scale (not shown). (This may be due to the increase in available potential energy due to the increase in the meridional temperature gradient, which in turn is likely due to the barotropic governor effect that occurs under increasing barotropic shear). Thus when friction is decreased in this model, the intrinsic phase-speed must decrease, and the conclusion that the poleward shift is categorically caused by the increase in phase-speed is less certain.

An increase in the eddy length scale is expected to have other repercussions. For instance, Charney and Drazin (1961) showed that only long waves are able to propagate from the troposphere into the high static stability environment of the stratosphere. An increase in the eddy length scale may therefore be expected to increase the pseudomomentum flux into the stratosphere. Pseudomomentum deposition in the stratosphere drives the Brewer-Dobson overturning, so it may be expected that this would increase if the eddy length scale increases. The Brewer-Dobson overturning is indeed projected to increase under increasing GHGs due to increased wave driving (Garcia and Randel 2008), but the cause of the increase in wave driving has not been identified. Further work may determine whether the increase in the eddy length scales in the CMIP3 output is a contributing factor.

Finally, to end on a note of prudence, by no means do we claim to have definitively determined the cause of the poleward shift of the jet streams in the CMIP3 runs, not the mention the real atmosphere. More work will clearly be needed to determine which, if any, of the mechanisms proposed thus far are quantitatively important for the projected poleward shift of the circulation under increasing GHGs, and only time will tell whether the shift occurs in the real atmosphere and by what mechanism.

Acknowledgments.

We gratefully acknowledge the revisions suggested by three anonymous reviewers. This work was partially supported by NOAA grant NA07OAR4310320.

REFERENCES

Anderson, J. L., V. Balaji, A. J. Broccoli, W. F. Cooke, T. L. Delworth, K. W. Dixon, L. J. Donner, K. A. Dunne, S. M. Freidenreich, S. T. Garner, R. G. Gudgel, C. T. Gordon, I. M. Held, R. S. Hemler, L. W. Horowitz, S. A. Klein, T. R. Knutson, P. J. Kushner, A. R. Langenhost, N. C. Lau, Z. Liang, S. L. Malyshev, P. C. D. Milly, M. J. Nath, J. J. Ploshay, V. Ramaswamy, M. D. Schwarzkopf, E. Shevliakova, J. J. Sirutis, B. J. Soden, W. F. Stern, L. A. Thompson, R. J. Wilson, A. T. Wittenberg, and B. L. Wyman, 2004: The new gfdl global atmosphere and land model am2-lm2: Evaluation with prescribed sst simulations. *Journal of Climate*, **17**, 4641–4673.

Barnes, E. A., D. L. Hartmann, D. M. W. Frierson, and J. Kidston, 2010: The effect of latitude on the persistence of eddy-driven jets. *Geophysical Research Letters*, **37**, L11804, doi:10.1029/2010GL043199.

Bengtsson, L., K. I. Hodges, and E. Roeckner, 2006: Storm tracks and climate change. *Journal of Climate*, **19**, 3518–3543.

Charney, J. G. and P. G. Drazin, 1961: Propagation of planetary-scale disturbances from the lower into the upper atmosphere. *Journal of Geophysical Research*, **66(1)**, 83–109.

Chen, G., 2007: *Mechanisms that control the latitude of jet streams and surface westerlies*. Ph.D. thesis, Princeton University.

Chen, G. and I. M. Held, 2007: Phase speed spectra and the recent poleward shift of southern hemisphere surface westerlies. *Geophysical Reseasrh Letters*, **34**, L21805.

Chen, G., I. M. Held, and W. A. Robinson, 2007: Sensitivity of the latitude of the surface westerlies to surface friction. *Journal of the Atmospheric Sciences*, **64**, 2899–2915.

Chen, G., J. Lu, and D. M. W. Frierson, 2008: Phase speed spectra and the latitude of surface westerlies: Interannual variability and global warming trend. *Journal of Climate*, **21**, 5942–5959.

Dritschel, D. G. and M. E. McIntyre, 2008: Multiple jets as PV staircases: The Phillips effect and the resilience of eddy-transport barriers. *Journal of the Atmospheric Sciences*, **65**, 855–874.

Edmon, H., B. Hoskins, and M. McIntyre, 1980: Eliassen-Palm cross sections for the troposphere. *Journal of the Atmospheric Sciences*, **37**, 2600–2616.

Feldstein, S. B., 2002: The recent trend and variance increase of the annular mode. *Journal of Climate*, **15**, 88–94.

Frierson, D. M. W., 2006: Robust increases in midlatitude static stability in simulations of global warming. *Geophysical Research Letters*, **33**, L24816.

Frierson, D. M. W., I. M. Held, and P. Zurita-Gotor, 2006: A gray-radiation aquaplanet moist GCM. part I: Static stability and eddy scale. *Journal of the Atmospheric Sciences*, **63**, 2548–2566.

Fyfe, J. C., G. J. Boer, and G. M. Flato, 1999: The Arctic and Antarctic oscillations and their projected changes under global warming. *Geophysical Research Letters*, **26**, 1601–1604.

Garcia, R. R. and W. J. Randel, 2008: Acceleration of the brewer-dobson circulation due to increases in greenhouse gases. *Journal of the Atmospheric Sciences*, **65**, 2731–2739.

Gerber, E. P., L. M. Polvani, and D. Ancukiewicz, 2008: Annular mode time scales in the intergovernmental panel on climate change fourth assessment report models,. *Geophysical Research Letters*, **35**, L22707.

Gerber, E. P. and G. K. Vallis, 2007: Eddy-zonal flow interactions and the persistence of the zonal index. *Journal of the Atmospheric Sciences*, **64**, 3296–3311.

Govindasamy, B. and S. T. Garner, 1997: The equilibration of short baroclinic waves. *Journal of the Atmospheric Sciences*, **54**, 2850–2871.

Haigh, J. D., M. Blackburn, and R. Day, 2005: The response of tropospheric circulation to perturbations in lower-stratospheric temperature. *Journal of Climate*, **18**, 3672–3685.

Hartmann, D. L., J. M. Wallace, V. Limpasuvan, D. W. J. Thompson, and J. R. Holton, 2000: Can ozone depletion and global warming interact to produce rapid climate change? *Proceedings of the National Academy of Sciences of the United States of America*, **97**, 1412–1417.

Hayashi, Y., 1979: A generalized method of resolving disturbances into progressive and retrogressive waves by space fourier and time cross-spectral analyses. *Journal of the Meteorological Society of Japan*, **41**, 125–128.

Held, I. M., 1982: On the height of the tropopause and the static stability of the troposphere. *Journal of the Atmospheric Sciences*, **39**, 412–417.

Held, I. M. and P. J. Phillips, 1987: Linear and nonliear barotropic decay on the sphere. *Journal of the Atmospheric Sciences*, **44**, 200–207.

Held, I. M. and M. J. Suarez, 1994: A proposal for the intercomparison of the dynamical cores of atmospheric general circulation models. *Bulletin of the American Meteorological Society*, **75**, 1825–1830.

Hurrell, J. W., 1996: Influence of variations in extratropical wintertime teleconnections on northern hemisphere temperature. *Geophysical Research Letters*, **23**, 665–668.

Johanson, C. and Q. Fu, 2008: Hadley cell widening: model simulations versus observations. *Submitted to Journal of Climate*.

Kalnay, E., M. Kanamitsu, R. Kistler, W. Collins, D. Deaven, L. Gandin, M. Iredell, S. Saha, G. White, J. Woollen, Y. Zhu, M. Chelliah, W. Ebisuzaki, W. Higgins, J. Janowiak, K. C. Mo, C. Ropelewski, J. Wang, A. Leetmaa, R. Reynolds, R. Jenne, and D. Joseph, 1996: The NCEP/NCAR 40-year reanalysis project. *Bulletin of the American Meteorological Society*, **77**, 437–471.

Kidston, J., S. M. Dean, J. A. Renwick, and G. K. Vallis, 2010a: A robust increase in the eddy length scale in the simulation of future climates. *Geophysical Research Letters*, **37**, L03806.

Kidston, J., J. A. Frierson, D. M. W. Renwick, and G. K. Vallis, 2010b: Observations, simulations, and dynamics of jet stream variability and annular modes. *Submitted, Journal of Climate*, **22**, In Press.

Kidston, J. and E. P. Gerber, 2010: Intermodel variability of the poleward shift of the austral jet stream in the CMIP3 integrations linked to biases in 20$^{\mathrm{th}}$ century climatology. *Geophysical Research Letters*, **37**, L09708, doi:10.1029/2010GL042873.

Kidston, J. and G. K. Vallis, 2010: The relationship between the latitude and width of the eddy-driven jet. *Geophysical Research Letters*, **In Press**, doi:10.1029/2010GL044849.

Kushner, P. J., I. M. Held, and T. L. Delworth, 2001: Southern hemisphere atmospheric circulation response to global warming. *Journal of Climate*, **14**, 2238 2249.

Lorenz, D. J. and E. T. DeWeaver, 2007: Tropopause height and zonal wind response to global warming in the IPCC scenario integrations. *Journal of Geophysical Research.*, **112**, D10119.

Lu, J., G. Chen, and D. M. W. Frierson, 2008: Response of the zonal mean atmospheric circulation to El Niño versus global warming. *Journal of Climate*, **21**, 5835–5851.

Marshall, G. J., 2003: Trends in the southern annular mode from observations and reanalyses. *Journal of Climate*, **16**, 4134–4143.

Meehl, G. A., C. Covey, T. Delworth, M. Latif, J. F. B. McAvaney, B.and Mitchell, R. J. Stouffer, and K. E. Taylor, 2007a: The WCRP CMIP3 multi-model dataset: A new era in climate change research. *Bulletin of the American Meteorological Society*, **88**, 1383–1394.

Meehl, G. A. and C. Tebaldi, 2004: More intense, more frequent, and longer lasting heat waves in the 21st century. *Science*, **305**, 994.

Meehl, G. T. S., W. Collins, P. Friedlingstein, A. Gaye, J. Gregory, A. Kitoh, R. Knutti, J. Murphy, A. Noda, S. Raper, I. Watterson, A. Weaver, and Z.-C. Zhao, 2007b: *Global Climate Projections. In: Climate Change 2007: The Physical Science Basis. Contribution of Working Group I to the Fourth Assessment Report of the Intergovernmental Panel on Climate Change.*. Cambridge University Press, Cambridge, United Kingdom and New York, NY, USA.

Miller, R. L., G. A. Schmidt, and D. T. Shindell, 2006: Forced annular variations in the 20^{th} century intergovernmental panel on climate change fourth assessment report models. *Journal of Geophysical Research-Atmospheres*, **111**.

Murphy, B. and B. Timbal, 2008: A review of recent climate variability and climate change in southeastern australia. *International Journal of Climatology*, **28, 7**, 859–879.

Orlanski, I., 2003: Bifurcation in eddy life cycles: Implications for storm track variability. *Journal of the Atmospheric Sciences*, **60**, 993–1023.

Ostermeier, G. M. and J. M. Wallace, 2003: Trends in the north atlantic oscillation-northern hemisphere annular mode during the twentieth century. *Journal of Climate*, **16**, 336–341.

Randel, W. J. and I. M. Held, 1991: Phase speed spectra of transient eddy fluxes and critical layer absorption. *Journal of the Atmospheric Sciences*, **48**, 688–697.

Rhines, P., 1975: Waves and turbulence on a beta-plane. *J. Fluid Mech.*, **69**, 417–443.

Son, S.-W., L. M. Polvani, D. W. Waugh, H. Akiyoshi, R. Garcia, D. Kinnison, S. Pawson, E. Rozanov, T. G. Shepherd, and K. Shibata, 2008: The impact of stratospheric ozone recovery on the southern hemisphere westerly jet. *Science*, **320**, 1486–1489.

Stott, P. A., D. A. Stone, and M. R. Allen, 2004: Human contribution to the european heatwave of 2003. *Nature*, **432**, 610614.

Thompson, D. W. J. and S. Solomon, 2002: Interpretation of recent southern hemisphere climate change. *Science*, **296**, 895–899.

Thompson, D. W. J., J. M. Wallace, and G. C. Hegerl, 2000: Annular modes in the extratropical circulation. part ii: Trends. *Journal of Climate*, **13**, 1018–1036.

Thorncroft, C. D., B. J. Hoskins, and M. E. McIntyre, 1993: Two paradigms of baroclinic-wave life-cycle behaviour. *Quarterly Journal of the Royal Meteorological Society*, **119**, 17–55.

Trenberth, K., P. Jones, P. Ambenje, R. Bojariu, D. Easterling, A. K. Tank, D. Parker, F. Rahimzadeh, J. Renwick, M. Rusticucci, B. Soden, and P. Zhai, 2007: *Observations: Surface and Atmospheric Climate Change. In: Climate Change 2007: The Physical Science Basis. Contribution of Working Group I to the Fourth Assessment Report of the Intergovernmental Panel on Climate Change*. Cambridge University Press, Cambridge, United Kingdom and New York, NY, USA.

Vallis, G. K., 2006: *Atmospheric and Oceanic Fluid Dynamics: Fundamentals and Large-Scale Circulation.*. Cambridge University Press.

Vallis, G. K. and M. E. Maltrud, 1993: Generation of mean flows and jets on a beta plane and over topography. *Journal of Physical Oceanography*, **23**, 1346–1362.

Welch, W. T. and K.-K. Tung, 1998: On the equilibrium spectrum of transient waves in the atmosphere. *Journal of the Atmospheric Sciences*, **55**, 2833–2851.

Williams, G. P., 2006: Circulation sensitivity to tropopause height. *Journal of the Atmospheric Sciences*, **63**, 1954–1961.

Yin, J. H., 2005: A consistent poleward shift of the storm tracks in simulations of 21^{st} century climate. *Geophysical Research Letters*, **32**, 1–4.

List of Figures

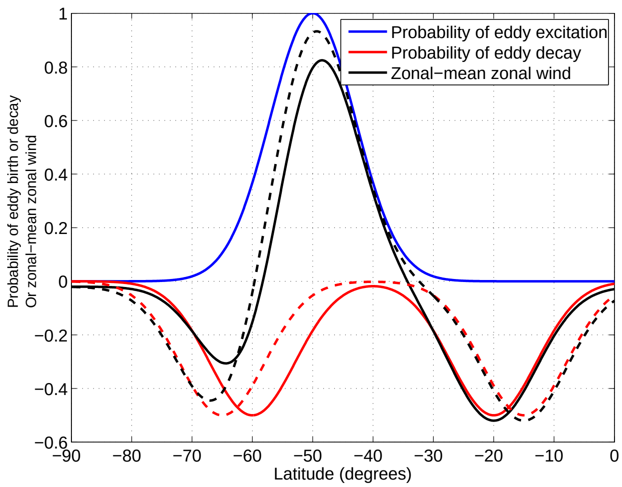

FIG. 1. A schematic of the proposed mechanism for how the increase in the eddy length scale may effect a poleward shift of the surface westerlies. The probability of exciting an eddy is shown by the blue line. The probability of an eddy decaying in the control (future) is shown by the red solid (dashed) line. The zonal wind speed is the sum of these probabilities (black lines), so that latitudes that are a net source of eddies have westerlies, and latitudes that are a net sink of eddies have easterlies. The values in the future are shown by the dashed lines.

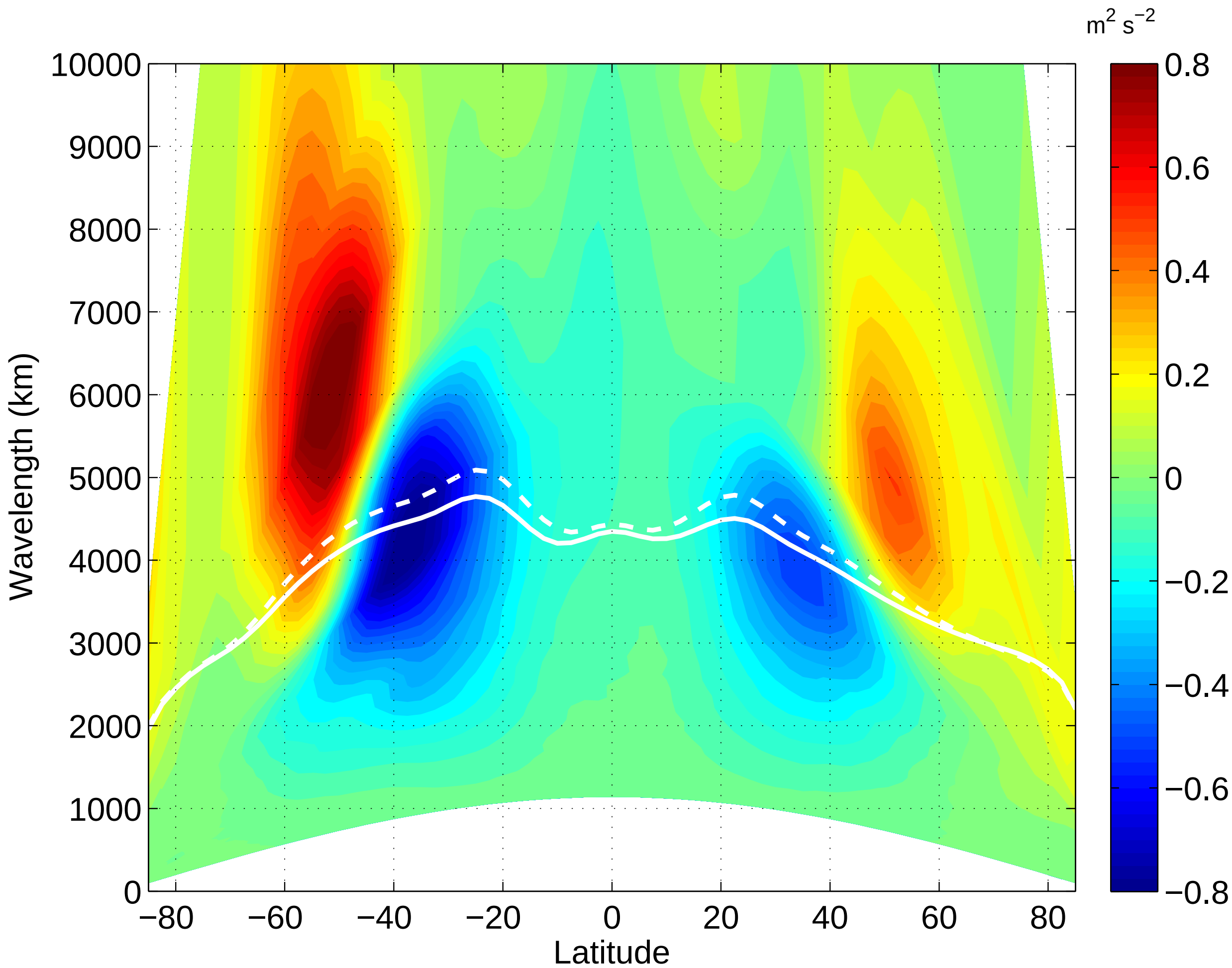

FIG. 2. The difference between the ensemble-mean eddy kinetic energy at 300 hPa in the 20C3M simulations (1981-2000) and the A2 simulations (2081-2100) in the Coupled Model Intercomarison Phase 3 (CMIP3). Also shown is the ensemble-mean eddy length scale ($L(\phi)$) for the 20C3M runs (solid line) and A2 runs (dashed line). The individual models used to compute the ensemble statistics are named bccr_bcm2_0, cccma_cgcm3_1, cnrm_cm3, csiro_mk3_5, gfdl_cm2_0, gfdl_cm2_1, giss_model_e_r, inmcm3_0, ipsl_cm4, miroc3_2_medres, mpi_echam5 and mri_cgcm2_3_2a.

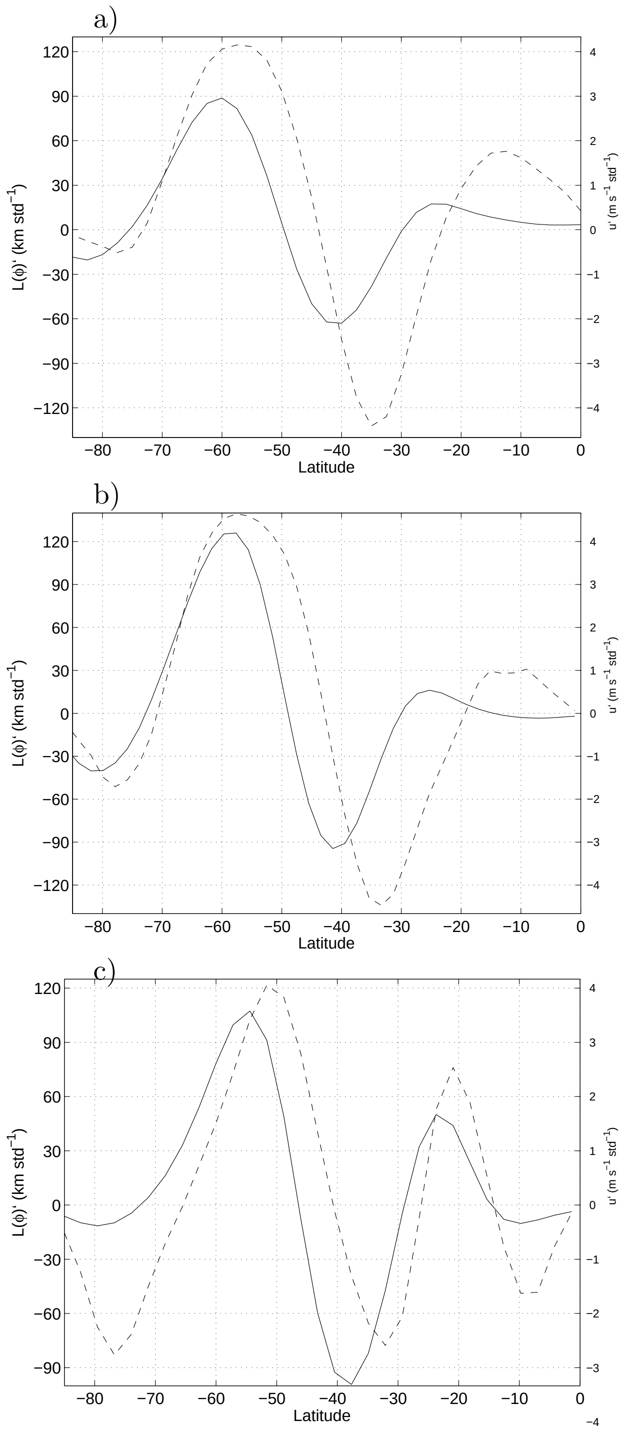

FIG. 3. Regression coefficient for the zonal-mean zonal wind ($\bar{u}$, solid line) and Ł(ϕ) (dashed line) with the standardized southern annular mode (SAM) index (see text) for: (a) the NCEP/NCAR reanalysis; (b) the 20C3M simulation in the gfdl_cm2_1 GCM; (c) the GFDL dynamical core.

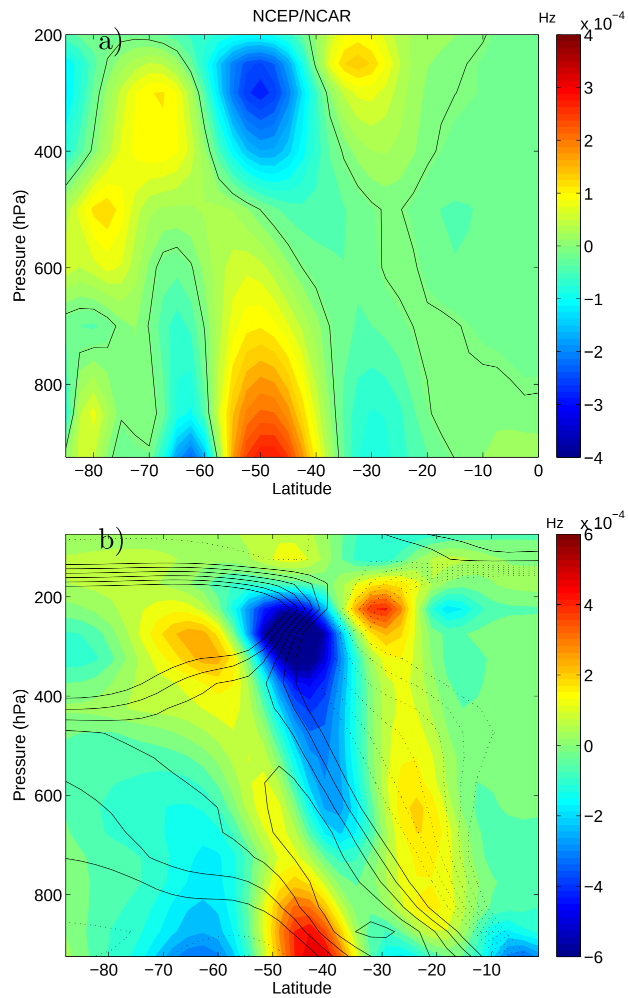

FIG. 4. Regression coefficient for the zonal-mean buoyancy frequency (N) and PC1: (a) the NCEP/NCAR reanalysis; (b) the GFDL dynamical core. Also shown in (b) are contours of the difference between N and the average N (at that pressure level). Contours are every $5{*}10^{-4}$ s^{-1} with negative contours dashed, positive contours solid, and the zero contour omitted.

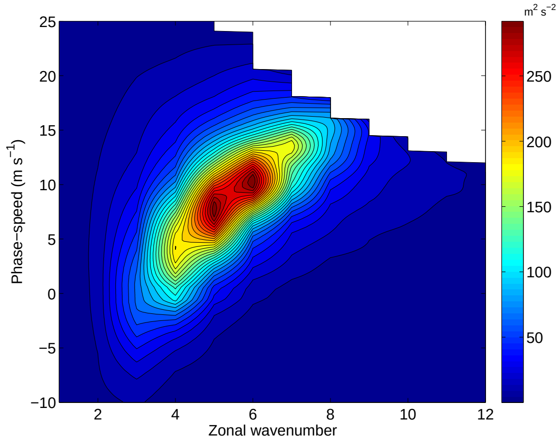

FIG. 5. The eddy kinetic energy of the meridional component of wind-speed as a function of zonal wavenumber and phase-speed. The data are from the gfdl_cm2_1 model, and are on the 300 hPa surface, at the approximate latitude of the eddy-driven jet of 51°S

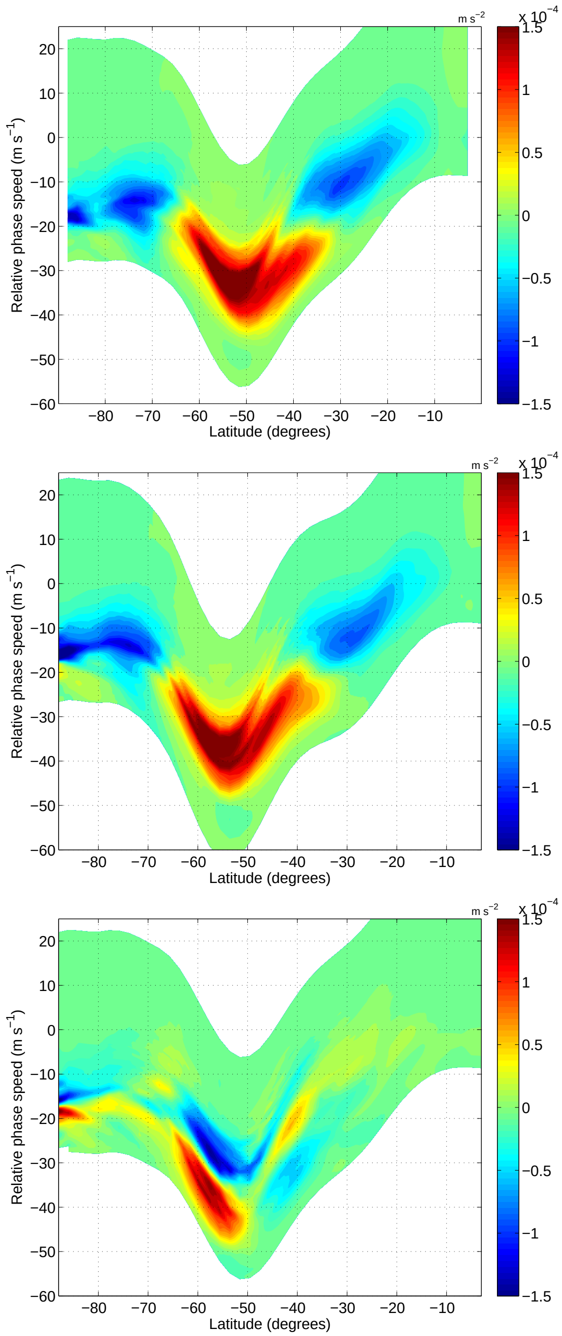

FIG. 6. The climatological momentum flux convergence in the gfdl_cm2_1 model at 300 hPa as a function of the relative eddy phase-speed (see text). Panel (a) shows NDJF output for the 20$^{\text{th}}$ century control. Panel (b) shows the same metric for the A2 scenario during 2080-2099. Panel (c) shows the difference between panels (a) and (b).

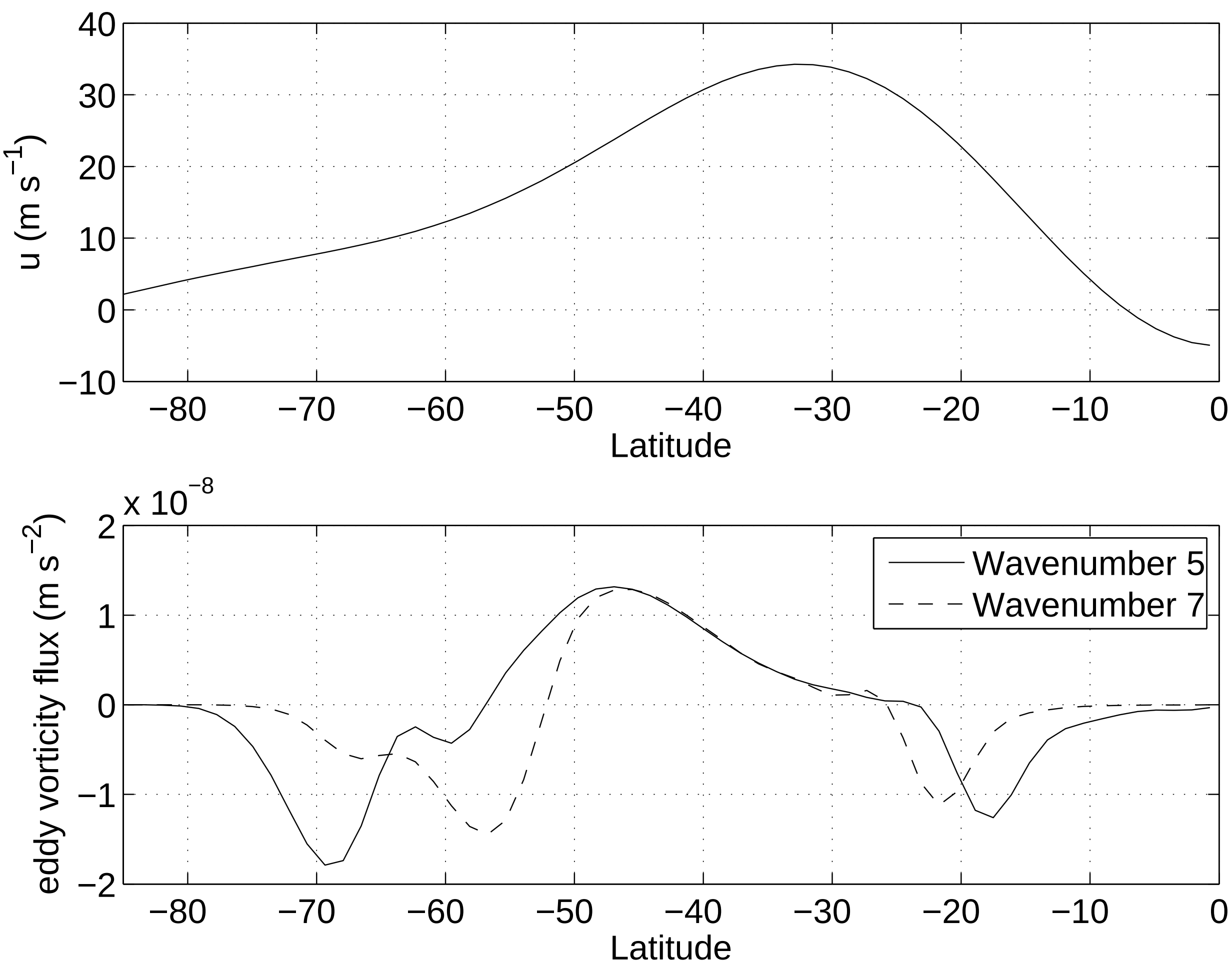

FIG. 7. Results of an initial value perturbation experiment using the barotropic model on a sphere (see text): (a) the zonal-mean zonal wind; (b) the total eddy vorticity flux ($\overline{v'\zeta'}$) after 20 days for initial zonal wavenumber 5 (k-5, solid line) and k-7 (dashed line).

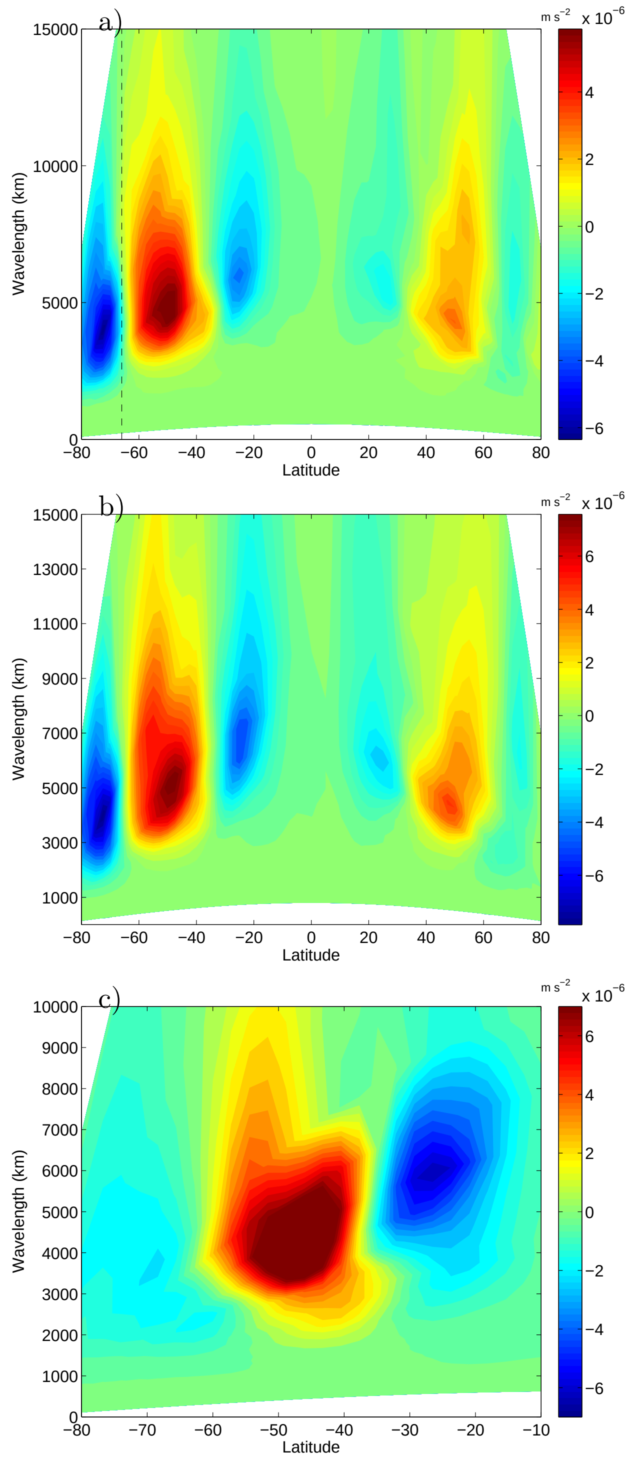

FIG. 8. Spectral decomposition of the time-mean $\overline{v'\zeta'}$ for the NCEP/NCAR reanalysis data (a); the 20C3m simulation in the gfdl_cm2_1 GCM (b); and the GFDL dynamical core (c).

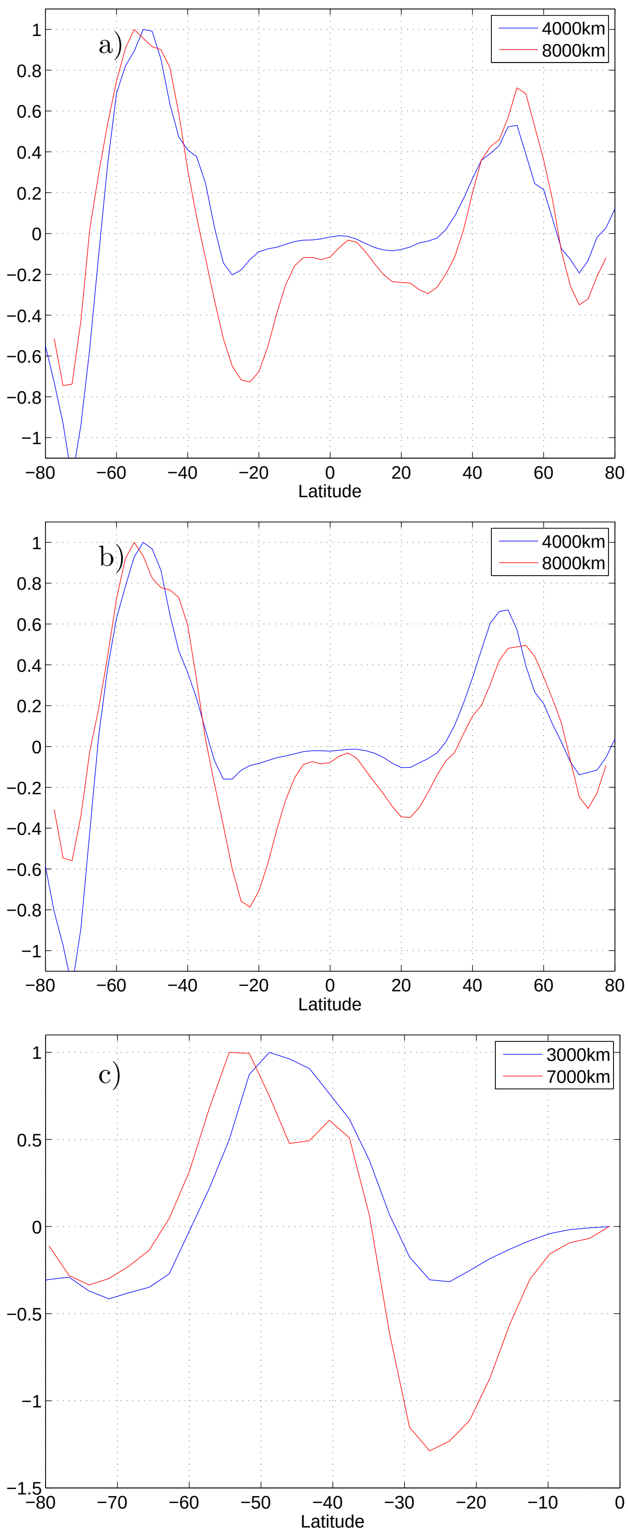

FIG. 9. A slice of the time-mean $\overline{v'\zeta'}$ show in Figure 8 for: (a) the NCEP/NCAR reanalysis; (b) the 20C3M simulation in the gfdl_cm2_1 GCM; (c) the GFDL dynamical core. The wavelength at which the slice was taken is given in the legend. The values have been normalized so that their maximum value is unity.

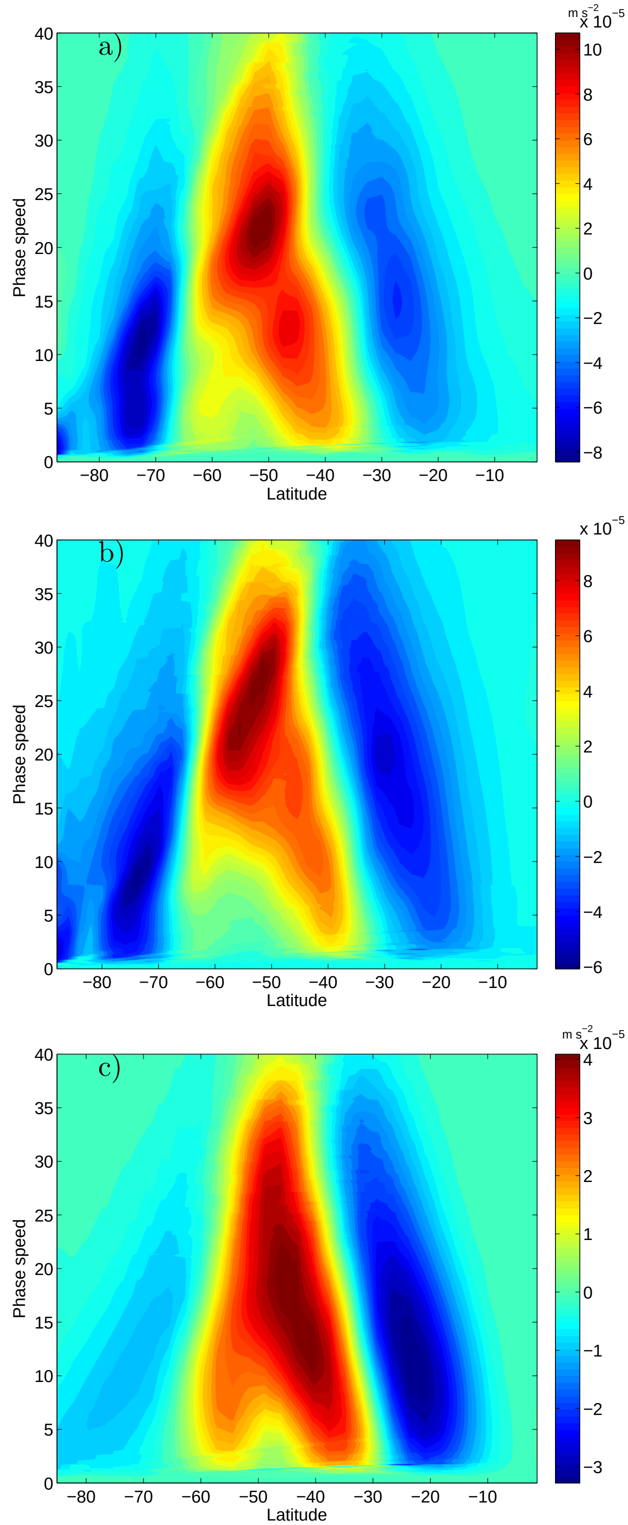

FIG. 10. Phase-speed decomposition of the time-mean $(\overline{v'\zeta'})$ for: (a) the NCEP/NCAR reanalysis; (b) the 20C3M simulation in the gfdl_cm2_1 GCM; (c) the GFDL dynamical core.

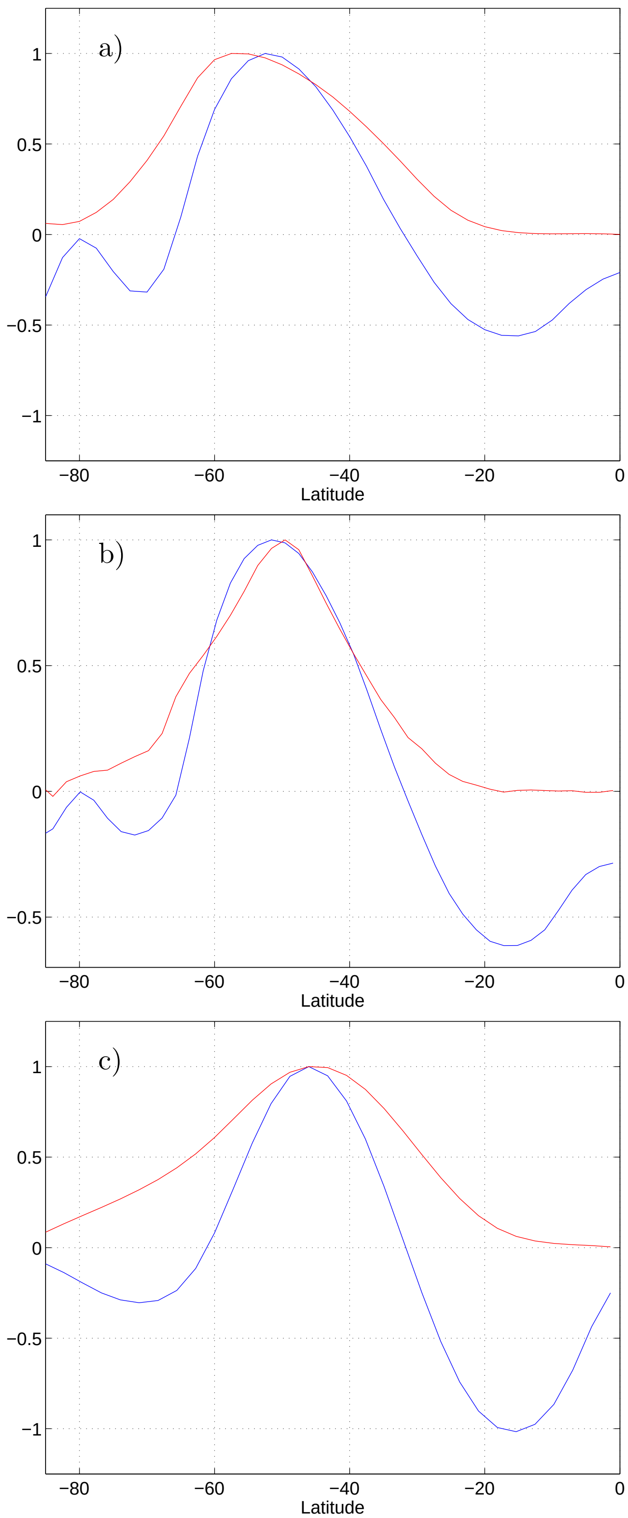

FIG. 11. The time-mean near surface $\bar{u}$ (blue line) and the time-mean vertical-mean poleward eddy heat flux (red line) for: (a) the NCEP/NCAR reanalysis; (b) the 20C3M simulation in the gfdl_cm2_1 GCM; (c) the GFDL dynamical core. Both fields have been normalized so that their maximum value is unity, and the eddy heat flux has been multiplied by minus one for comparison with the wind field.

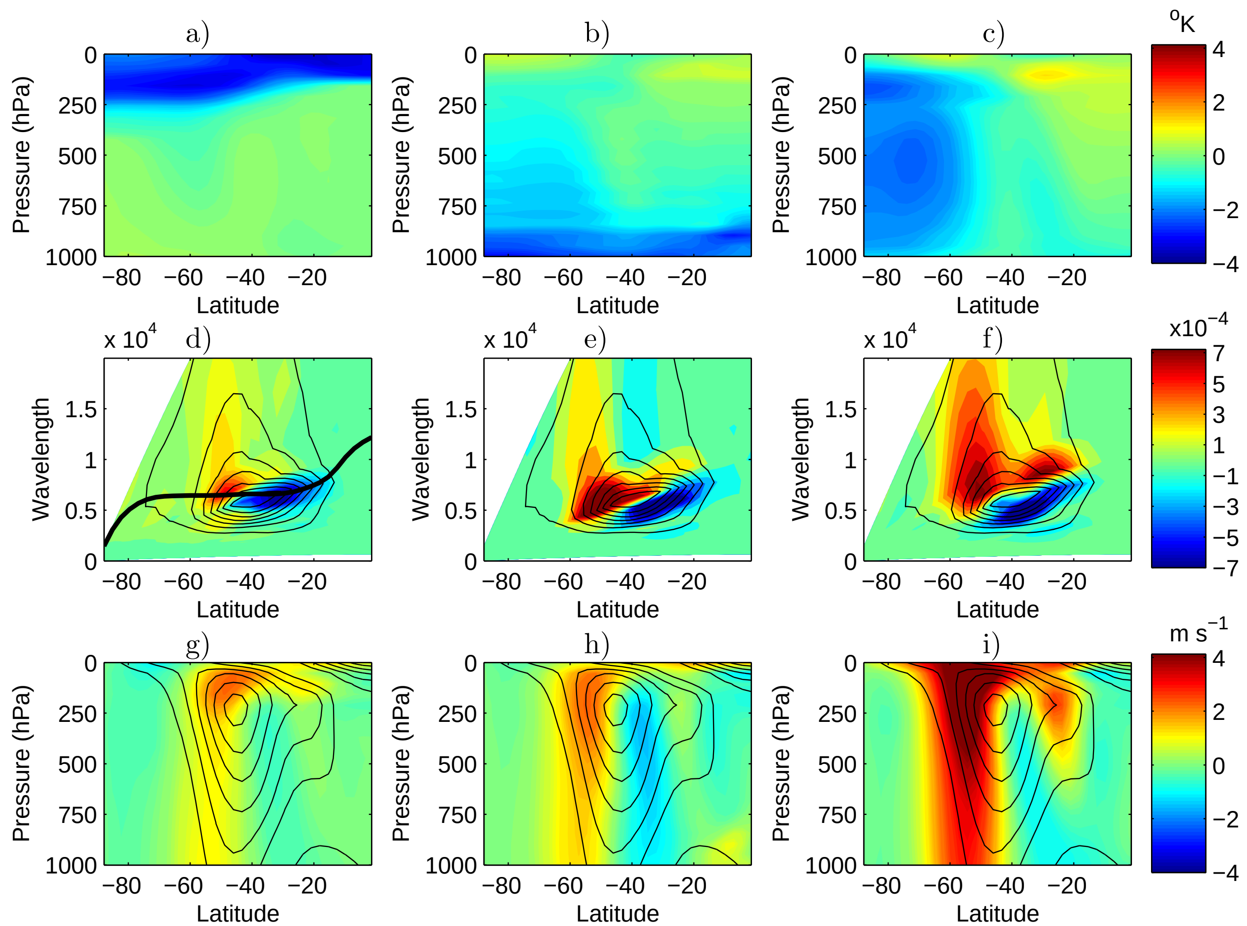

FIG. 12. The upper panels show the difference in zonal-mean temperature between the experiments and the control. The center row of panels shows the change in EKE as a function of wavelength and latitude 240 hPa. The contours are for the control run, starting at 0.1 with 0.1 interval. The shading is the difference between the experiment and the control run. The bold contour in the center left panel shows $L(\phi)$ for the control run. The bottom row of panels shows the zonal mean zonal wind in the control run as contours. The contour interval is ± 5 m s^{-1} with solid (dashed) contours representing positive (negative) values and the zero contour omitted. The shading is the difference between the experiments and the control run. The left column of panels corresponds to the experiment $H_{increased}$, where the stratospheric equilibrium (T_{eq}) was reduced by 3 K. The middle column corresponds to the experiment $N_{increased}$, where T_{eq} was reduced by 3 K in the lowest three model layers. The right column corresponds to the experiment $|\partial T/\partial y|_{increased}$, where the e-folding time of the Newtonian cooling was reduced from 40 days to 30 days.

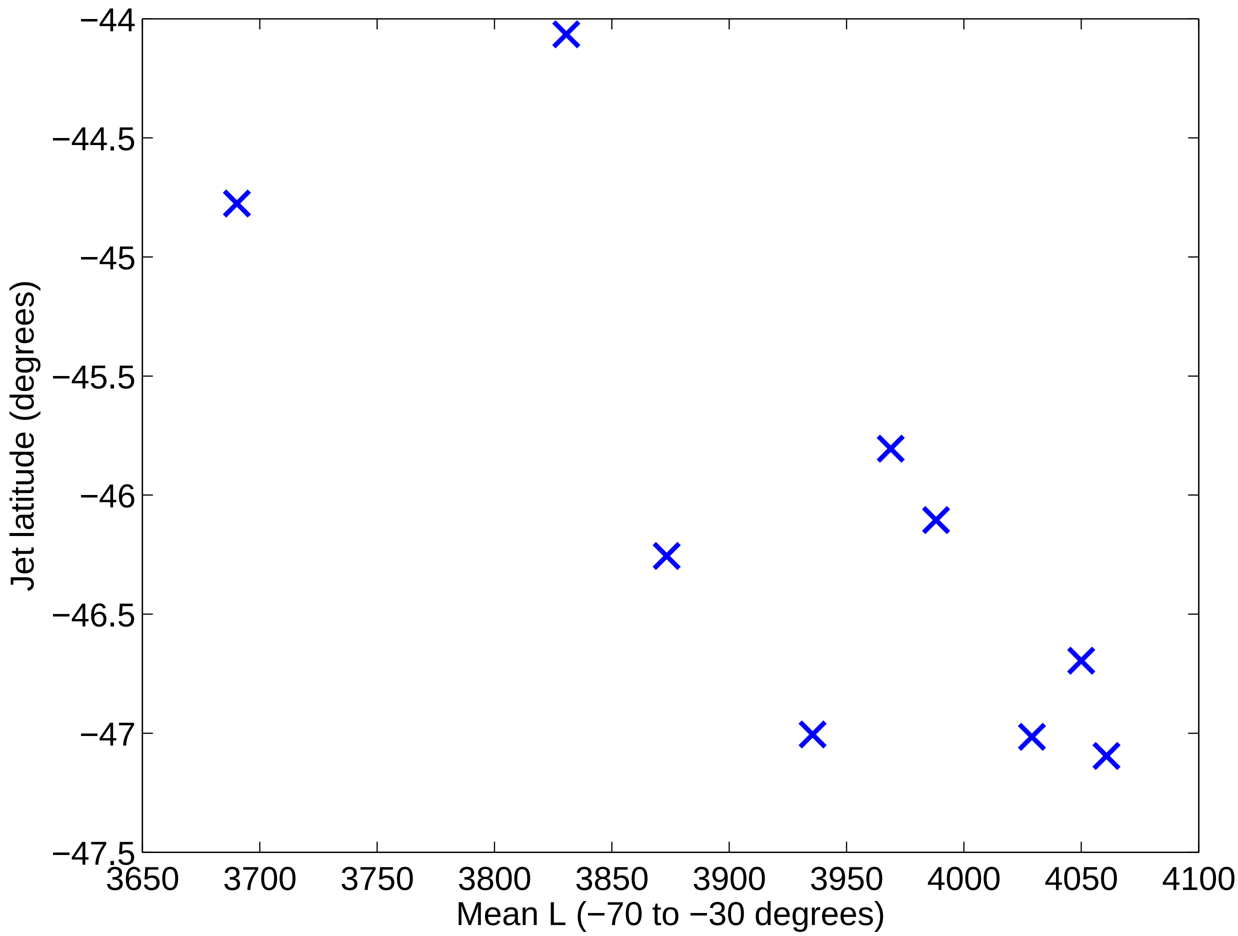

FIG. 13. The variation of jet-latitude with eddy wavelength (at 240 hPa) for 9 different experiments. In the experiments the e-folding time for the hyperdiffusivity operator was varied. The experiments are summarized in Table1.

List of Tables

Table 1. Summary of 9 experiments with the simplified GCM. The e-folding time for the hyperdiffusivity operator was set to the value in the first row. The second row shows the eddy length scale averaged between -70° and -25°S (see text) and the third row shows the latitude of the maximum surface westerlies (see text).

Damping time (days)	1/2	1/5	1/7	1/10	1/15	1/20	1/25	1/30	1/35
Mean length scale (km)	3690	3831	3873	3936	3969	3988	4029	4050	4061
Jet latitude (degrees)	-44.8	-44.1	-46.3	-47.0	-45.8	-46.1	-47.0	-46.7	-47.1